High-Conversion-Efficiency Optical Parametric Chirped-Pulse Amplification System Using Spatiotemporally Shaped Pump Pulses

Since its invention in the early 1990s,[1] optical parametric chirped-pulse amplification (OPCPA) has become an attractive alternative to Ti:sapphire-based regenerative amplifiers for producing millijoule-level broadband laser pulses for injection of high-energy, short-pulse lasers that operate at a 1-μm wavelength.[2–4] The primary advantage of OPCPA is the fact that only a single pass through several (~3 to 7) centimeters of material is required to provide broadband pulse-amplification factors as large as 10^8 with little or no gain narrowing. Due to its single-pass nature, pulses amplified using OPCPA do not have the prepulses that are commonly associated with regenerative amplifiers, and the fact that a minimal amount of material is required means that there is little *B*-integral accumulation in the amplification process. It has been noted, however, that the pump-to-signal conversion efficiency of the OPCPA process can be quite poor, especially for systems pumped by commercial, *Q*-switched lasers, [5] Thus if several hundred millijoules of OPCPA output are desired at moderate repetition rates (1 to 10 Hz), pump lasers providing of the order of 5 J of energy at these repetition rates would be required. In addition, if high OPCPA output stability is also required, the fact that OPCPA involves a nonlinear amplification process means that the pump laser must also have very good energy stability.

One approach to overcoming these concerns is to use a pump laser that is better suited to the OPCPA process. Since this process involves no energy storage, the amplification factor for a pulse at a given temporal and spatial position is determined by the pump intensity at that particular spatiotemporal location. This has several implications: First, careful tailoring of the pump and seed spatiotemporal profiles is required to achieve high optical parametric amplification (OPA) conversion efficiency.[6,7] Second, even slight variations in the pump intensity can result in large amplification-factor fluctuations, potentially leading to significant spatial and spectral modulation and large overall energy fluctuations in the amplified broadband output pulse. It has been shown that, for a narrow range of pump intensities and a particular interaction length, saturation in the OPA process can be observed, reducing the amplification-factor fluctuations to a value similar to or lower than that of the pump.[8,9] As a consequence, in addition to careful design of the OPA itself, it is also important that the pump intensity profile be carefully controlled in both space and time to achieve efficient and stable operation of the parametric amplifier.

Much of the previous OPCPA work reported in the literature was conducted using pump lasers that offered limited control over the pumping pulse characteristics.[3,4,10,11] In this article, we experimentally demonstrate that improved control over the temporal and spatial profiles of the pump laser significantly increases the efficiency of the OPA process. We emphasize the temporal and spatial aspects of the pump that provide optimal pumping conditions, leading to both efficient and stable OPCPA output characteristics.

To optimize the OPCPA conversion efficiency and stability, a three-dimensional modeling code was developed that predicts the output of an OPCPA system given arbitrary pump and seed input energies and spatiotemporal profiles. This model, the details of which are described elsewhere,[12] was used to determine both the optimal pump spatiotemporal profile and the OPCPA configuration. Optimal conversion efficiency can be obtained with a uniform rate of energy transfer from the pump to the signal and idler, homogeneously depleting the pump in space and time. In our setup, a pump temporal profile that is flat in time with fast rise and fall times and a full width at half maximum (FWHM) that is roughly equivalent to that of the seed pulse is required. The spatial profile of the pump laser should be high-order super-Gaussian with a FWHM that is comparable to that of the seed pulse. As it is amplified, the originally Gaussian spatiotemporal profile of the seed is significantly sharpened due to the high gain of the OPA process. Thus when the amplification process begins to saturate, the spatiotemporal profiles of the seed and pump are well matched, improving energy extraction. Lithium triborate (LBO) was chosen as the OPA nonlinear medium because of its relatively high nonlinearity, high angular acceptance, and low walkoff between the pump beam (extraordinary wave) and the seed

beam (ordinary wave). The input pump intensity was limited primarily by the measured damage threshold of the antireflective coatings on the OPA crystals, so the model was used to select the crystal lengths that provided both high conversion efficiency and an amplified broadband pulse whose energy and spatial profile fluctuations were minimized.

A diagram of the experimental OPCPA setup is shown in Fig. 93.25. The OPA pump laser, shown in the shaded box, consists of a master oscillator, a temporal pulse-shaping system, a diode-pumped Nd:YLF regenerative amplifier, spatial beam shaping, a double-passed Nd:YLF power amplifier, and frequency doubling. The oscillator is a diode-pumped, single-longitudinal-mode Nd:YLF laser producing ~100-nJ pulses at 1.053 μm with a 300-Hz repetition rate.[13] The output of the oscillator is sent into an aperture-coupled-stripline (ACSL) temporal-pulse-shaping system, which can be configured to provide nearly arbitrary temporal pulse shapes for pulses up to 4 ns in duration.[14] The temporally shaped pulse is then amplified from ~50 pJ to 3 mJ in a diode-pumped, Nd:YLF regenerative amplifier.[15] The output of the regenerative amplifier is spatially expanded and apodized using a serrated-tooth apodizer to produce a 5-mm-FWHM beam that has a flat spatial profile at the output of the pump laser. The apodized pulse is then amplified from ~400 μJ to 40 mJ in a two-pass, flashlamp-pumped, 7-mm Nd:YLF power amplifier operating at 5 Hz. The output of the amplifier is relay imaged to a 3-mm beta-barium borate (BBO) frequency-doubling crystal, producing 526.5-nm pulses with energies as high as 25 mJ. A Pellin–Broca prism separates the second-harmonic light from the unconverted 1.053-μm light so that the latter does not serve as a seed for the OPA. The output of the BBO is then relay imaged to the OPA crystals.

As discussed above, optimizing the conversion efficiency of our OPCPA system requires a constant-intensity pump pulse with a temporal duration that is of the order of that of the seed. As shown in Fig. 93.26(a), temporally flat, 1-ns pulses with a 10 to 90 rise time of ~160 ps are produced at the output of the BBO doubling crystal. The time-integrated spatial profile of the pump laser, measured at the input to the OPA, is presented

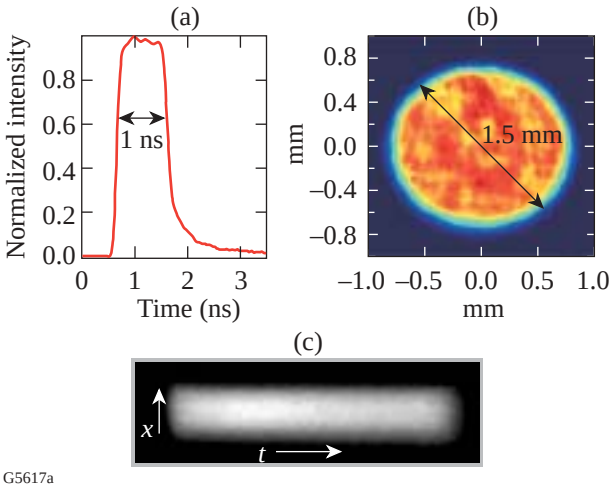

Figure 93.26
(a) 1-ns FWHM square temporal profile of the OPA pump laser; (b) spatial profile of the OPA pump laser; (c) streak camera measurement of the spatiotemporal profile of the pump showing little spatiotemporal coupling.

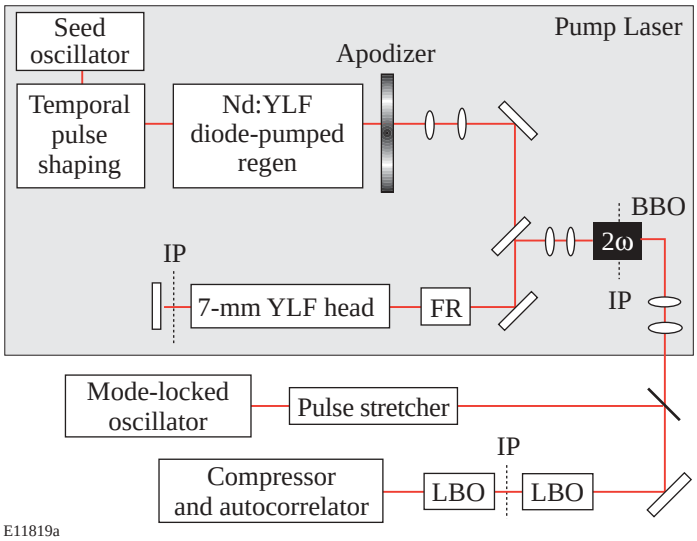

Figure 93.25
Diagram of the OPCPA experimental setup. The shaded box includes all of the components of the OPA pump laser. FR: Faraday rotator, IP: image plane; BBO: beta-barium borate; LBO: lithium triborate.

in Fig. 93.26(b). This beam has a tenth-order super-Gaussian spatial profile with a FWHM that is approximately equal to the spatial FWHM of the seed pulse. Because OPCPA is an instantaneous process, variations in the spatial profile of the pump over its temporal duration (spatiotemporal coupling) can lead to a reduction in conversion efficiency.[4] Figure 93.26(c) shows the spatiotemporal profile of the pump pulse as measured by a streak camera, demonstrating that there is no spatiotemporal coupling in the OPA pump pulse.

The broadband seed laser for the OPCPA system is a mode-locked, Nd:glass laser (Time-Bandwidth Products, Inc.) producing pulses with a center wavelength of 1.053 μm and a FWHM bandwidth of ~6 nm. The laser operates at a repetition rate of 76 MHz and is synchronized to an external master clock that also controls the OPA pump laser's master oscillator and pulse-shaping system. The jitter between the broadband seed and pump lasers, which can lead to output energy and temporal profile fluctuations, was measured to be less than 23 ps peak-to-valley and thus does not affect the stability of the OPCPA output. The 160-mW output of the seed laser is temporally stretched to ~700 ps in a double-passed, Öffner-triplet-based pulse stretcher,[16,17] providing ~800 pJ of seed energy at the OPA input with a Gaussian spatial and temporal profile.

The OPA consists of two wedged (2°), 5 × 5-mm-clear-aperture LBO crystals with lengths of 25 and 23 mm cut at 11.8° to allow type-I angular phase matching. The crystals have dielectric antireflective coatings provided by the vendor (Conex Systems, Inc.). The pump and temporally stretched seed beams have a FWHM of ~1.5 mm, providing a maximum pump intensity of ~1.1 GW/cm^2. The two LBO crystals are used in a walkoff-compensated configuration[18] with a ~4-mm air gap between them. This gap introduces a negligible amount of dephasing that does not affect the conversion process. The angle between the pump and seed pulses is 0.5°, which allows the signal and idler beams to be separated after the OPA process.

Figure 93.27 shows the conversion efficiency of the two-crystal OPCPA system as a function of pump energy. At maximum conversion efficiency, 17.7 mJ of pump energy produces 5.1 mJ of amplified signal energy, providing an overall gain of greater than 6×10^6 and a conversion efficiency of 29%. As demonstrated by the solid curve in Fig. 93.27, there is excellent agreement between modeling and experimental results. In addition to maximizing conversion efficiency, the OPCPA system was designed to minimize output-energy fluctuations. As shown in the inset table in Fig. 93.27, at the point of maximum conversion efficiency, the energy stability of the OPCPA output is 1.6% rms (measured over 100 shots) and is actually better than that of the pump. This improvement in output stability over that of the pump was predicted previously[8] and was achieved by carefully designing our OPA so that, at its output, energy in the signal just begins to reconvert into pump energy. We believe that this system demonstrates a significant improvement in output stability beyond systems previously reported in the literature.

The spectra of the input, stretched seed pulse and the amplified signal pulse are shown in Fig. 93.28(a). The FWHM of the amplified signal spectrum is approximately 8 nm, centered at ~1055 nm. Whereas the spectrum of the unamplified seed pulse is roughly Gaussian in shape, the shape of the amplified spectrum is square due to saturation in the OPCPA process. The amplified output of the OPCPA system is compressed in a double-passed, single-grating compressor.

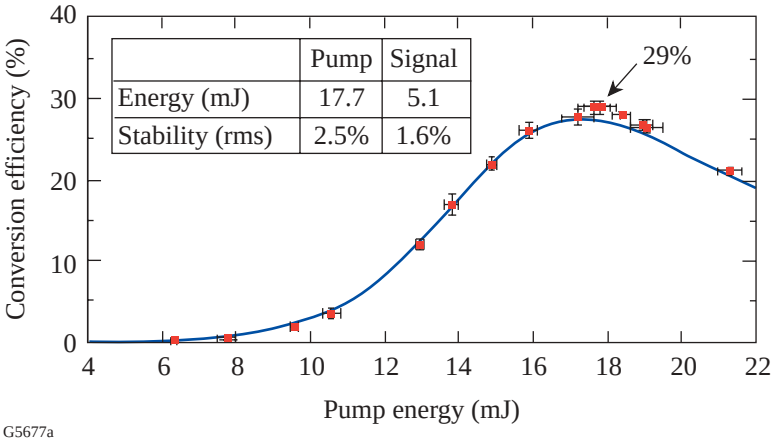

G5677a

Figure 93.27
Conversion efficiency as a function of pump energy. Solid curve shows model predictions with the squares representing experimentally measured values. Error bars show fluctuations in measured energies. Inset chart shows pump and signal energies and stabilities at the 29% conversion efficiency point.

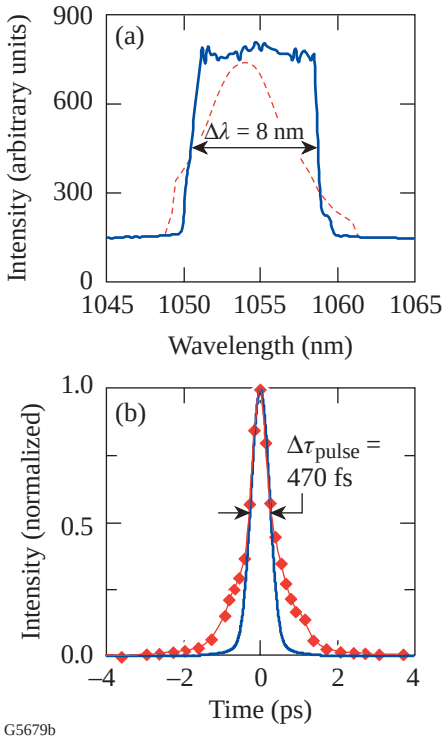

Figure 93.28
(a) Spectra of stretched seed pulse (dashed) and amplified signal pulse (solid). Clipping in the seed-pulse spectrum is due to the finite extent of the stretcher optics. (b) Measured autocorrelation (diamonds) of the amplified signal shown along with an autocorrelation trace (solid line) calculated from a fast Fourier transform (FFT) of the spectrum of the amplified signal shown in part (a). The wings in the measured autocorrelation are also present without OPCPA amplification, indicating that they are due to spectral phase errors in the stretcher–compressor combination.

The autocorrelation at the output of the pulse compressor, as measured with a scanning autocorrelator, is shown in Fig. 93.28(b). Using the measured spectra to estimate the transform-limited pulse width, we estimate the temporal duration (FWHM) of the compressed, amplified signal to be 470 fs, which is approximately 1.3 times the Fourier transform limit. Without amplification, the stretched and recompressed seed autocorrelation trace contains wings that are similar to those shown in Fig. 93.28(b). We thus believe that these wings are due to the uncompensated spectral phase in our stretcher–compressor combination and not the OPCPA process itself.

One of the advantages of an OPA is the fact that any aberrations in the pump spatial profile are transferred to the idler beam. Thus, the signal-beam quality is not degraded in the OPA. We measured the far field of our amplified signal beam at the focus of a 500-mm-focal-length lens with a 12-bit beam analyzer (Spiricon LBA 500PC and Cohu 4800 CCD camera). By comparing the FWHM of the Fourier transform of the measured near-field profile with that of the measured far field, we determined that the amplified-signal-beam FWHM is ~1.3 times the diffraction limit in the horizontal direction and ~1.1 times the diffraction-limited width in the vertical direction. These numbers match closely with those measured for the stretched seed pulse, indicating that the OPA did not introduce additional phase errors to the spatial profile of the amplified pulse.

The maximum pump-to-signal conversion efficiency possible in a degenerate OPA such as the one presented here is 50%. In our experiment, the conversion efficiency is limited by a number of factors including the finite slopes of the spatiotemporal profile of the pump pulse, walk-off between the seed and pump, and noise in the spatiotemporal profile. Our simulations show that if we are able to decrease the rise time of the temporal profile to ~50 ps and increase the order of the super-Gaussian spatial profile to 30, we could increase the conversion efficiency of our system to approximately 40%. We have also designed a new OPCPA system containing a two-crystal preamplifier and a single-crystal power amplifier that will be able to generate higher energies while increasing the overall system conversion efficiency to greater than 40%.[12]

We have demonstrated an OPCPA system that uses a spatiotemporally shaped pump pulse to maximize the conversion efficiency of the OPCPA process. This system produces 5 mJ of amplified signal at a 5-Hz repetition rate with a pump-to-signal conversion efficiency of 29%. To our knowledge, this is the highest conversion efficiency ever achieved in an OPCPA system. In addition to high conversion efficiency, the system output is highly stable with an rms stability of 1.6%, which is actually better than that of the pump laser.

ACKNOWLEDGMENT

This work was supported by the U. S. Department of Energy Office of Inertial Confinement Fusion under Cooperative Agreement No. DE-FC03-92SF19460, the University of Rochester, and the New York State Energy Research and Development Authority. The support of DOE does not constitute an endorsement by DOE of the views expressed in this article.

REFERENCES

1. A. Dubietis, G. Jonusauskas, and A. Piskarskas, Opt. Commun. **88**, 437 (1992).

2. I. N. Ross *et al.*, Opt. Commun. **144**, 125 (1997).

3. J. Collier *et al.*, Appl. Opt. **38**, 7486 (1999).

4. I. Jovanovic *et al.*, Appl. Opt. **41**, 2923 (2002).

5. I. Jovanovic, C. A. Ebbers, and C. P. J. Barty, Opt. Lett. **27**, 1622 (2002).

6. I. A. Begishev *et al.*, Sov. J. Quantum Electron. **20**, 1100 (1990).

7. I. A. Begishev *et al.*, Sov. J. Quantum Electron. **20**, 1104 (1990).

8. S. K. Zhang *et al.*, Opt. Commun. **184**, 451 (2000).

9. M. J. Guardalben, J. Keegan, L. J. Waxer, and J. D. Zuegel, presented at the 2002 OSA Annual Meeting, Orlando, FL, 29 September–3 October 2002 (paper TuC5).

10. I. N. Ross *et al.*, Appl. Opt. **39**, 2422 (2000).

11. X. Yang *et al.*, Opt. Lett. **27**, 1135 (2002).

12. M. J. Guardalben, J. Keegan, L. J. Waxer, and J. D. Zuegel, "Optimization of a High-Conversion-Efficiency Optical Parametric Chirped-Pulse Amplification System" (in preparation).

13. A. V. Okishev and W. Seka, IEEE J. Sel. Top. Quantum Electron. **3**, 59 (1997).

14. M. D. Skeldon, A. V. Okishev, R. L. Keck, W. Seka, and S. Letzring, in *Third International Conference on Solid State Lasers for Application to Inertial Confinement Fusion*, edited by W. H. Lowdermilk (SPIE, Bellingham, WA, 1999), Vol. 3492, pp. 131–135.

15. A. V. Okishev, D. Battaglia, I. Begishev, and J. D. Zuegel, in *OSA Trends in Optics and Photonics (TOPS) Vol. 73, Conference on Lasers and Electro-Optics*, OSA Technical Digest (Optical Society of America, Washington, DC, 2002), pp. 365–366.

16. G. Cheriaux *et al.*, Opt. Lett. **21**, 414 (1996).

17. D. Du *et al.*, Opt. Lett. **20**, 2114 (1995).

18. D. J. Armstrong *et al.*, J. Opt. Soc. Am. B **14**, 460 (1997).